THE DETECTION OF SMALL-SCALE STRUCTURES IN PLANETARY SURFACE MATERIALS WITH GROUND-PENETRATING INSTRUMENTS.

G. Kargl[(1)], A. Zöhrer[(2)], N.I. Kömle[(3)], A.J. Ball[(4)], T.J. Ringrose[(5)], M.D. Paton[(6)], K.R. Atkinson[(7)], M.C. Towner[(8)], K.L. Kapper[(9)]

[(1)] Space Research Institute, Austrian Academy of Sciences, Schmiedlstr. 6, A-8042, Graz, Austria, Email: guenter.Kargl@oeaw.ac.at
[(2)] Space Research Institute, Austrian Academy of Sciences, Schmiedlstr. 6, A-8042, Graz, Austria, Email: alexander.zoehrer@oeaw.ac.at
[(3)] Space Research Institute, Austrian Academy of Sciences, Schmiedlstr. 6, A-8042, Graz, Austria, Email: norbert.koemle@oeaw.ac.at
[(4)]PSSRI, The Open University, Walton Hall, Milton Keynes, MK7 6AA, United Kingdom, Email: A.J. Ball@open.ac.uk
[(5)]PSSRI, The Open University, Walton Hall, Milton Keynes, MK7 6AA, United Kingdom, Email: T.J.ringrose@open.ac.uk
[(6)]PSSRI, The Open University, Walton Hall, Milton Keynes, MK7 6AA, United Kingdom, Email: m.paton@open.ac.uk
[(7)]PSSRI, The Open University, Walton Hall, Milton Keynes, MK7 6AA, United Kingdom, Email: k.r.atkinson@open.ac.uk
[(8)]PSSRI, The Open University, Walton Hall, Milton Keynes, MK7 6AA, United Kingdom, Email: m.c.towner@open.ac.uk
[(9)] Space Research Institute, Austrian Academy of Sciences, Schmiedlstr. 6, A-8042, Graz, Austria, Email: cadja@sbox.tugraz.at

ABSTRACT

The usage of mechanically ground-penetrating instruments can yield valuable information about layering and granularity on almost any extraterrestrial surface, as has recently been demonstrated with the Huygens probe [1]. We will demonstrate the kind of information that can be derived with the use of quasi-static and dynamic penetrometry sensors.
We will show examples of penetration experiments in preparation for future Mars lander instruments, and dynamic penetrations performed during the development and testing of the anchoring system of the Rosetta Philae lander. The paper will focus on the detection of small-scale structures and their signatures in a penetrometer signal, namely resonances forced by semi-regular scales (granularity) and boundary crossings (layers).
The study of resonant signatures allows an approximation of the average grain size distribution within the penetrated distance to be derived.

1 GENERAL SPECIFICATIONS

Penetrometry is the probing of a surface material via the insertion of a test projectile. We can generally divide between two major methods, which differ in the speed of insertion and the returned data.
These methods originate from terrestrial applications, which are quite common for engineering and geotechnical purposes.
Such measurements were proposed for various missions to the planet Mars, and are implemented on the Philae lander of the Rosetta mission to comet 67P/Churyumov-Gerasimenko [2]. The most successful application of such a method was the Huygens probe landing on Titan on 14. January 2005, where the ACC-E sensor of the Surface Science Package [3] delivered impact data from the first 5 cm of Titan's soil.

1.1 Quasi-static penetrometry

Quasi-static penetrometry is the slow insertion of a rod with a conical tip into a soil sample. A typical data set contains the record of the force necessary for penetrating the ground.
Together with the insertion speed mechanical parameters of the soil can be reconstructed via a soil model [4].
A dedicated penetrometry test facility for quasi-static experiments was set up at the Space Research Institute in Graz. With this facility we can perform experiments in Martian soil mechanical analogue materials with penetration speeds of about

Proc. '3rd International Workshop Planetary Probe', Anavyssos, Attiki, Greece, 27 June – 1 July 2005 (ESA SP-607, April 2006)

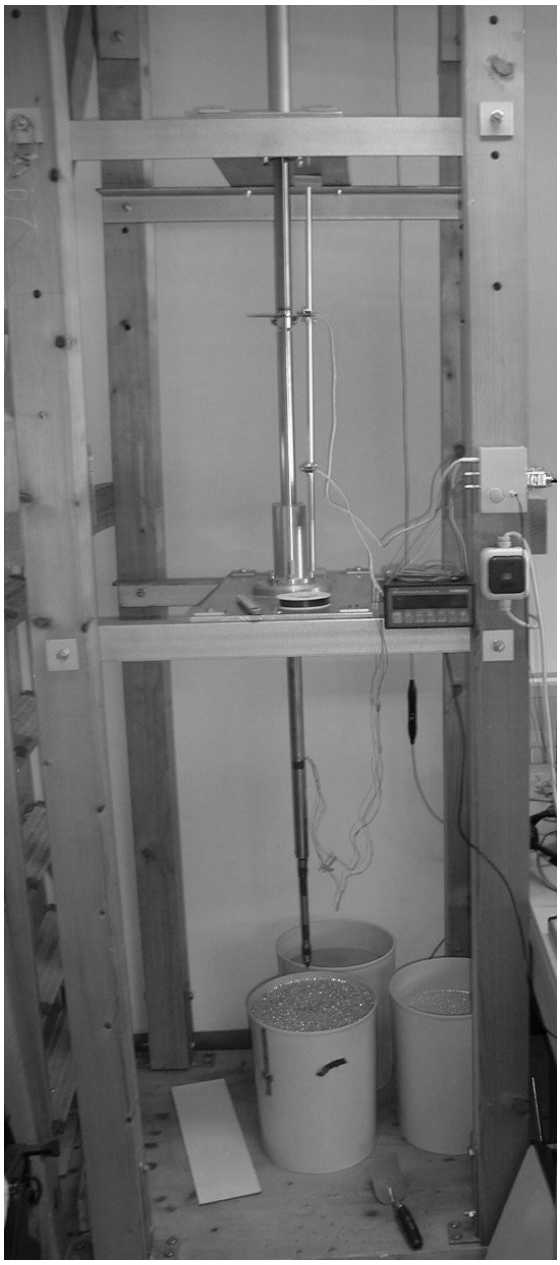

Figure 1 The penetrometry test facility in Graz used for quasi-static experiments in Martian soil analogues.

1.4 cms^{-1}, and a maximum depth of approximately 25 - 30 cm.

The selected Martian analogue materials include the JSC-Mars-1 palagonite from Hawaii and the Salten Skov iron precipitate from Denmark. Additionally we selected some local materials with a similar grain size distribution which were available in larger quantities, plus glass beads with ~1 and ~4 mm diameter as a calibration target. A more detailed description of all the sample materials used can be found in [4] and [5].

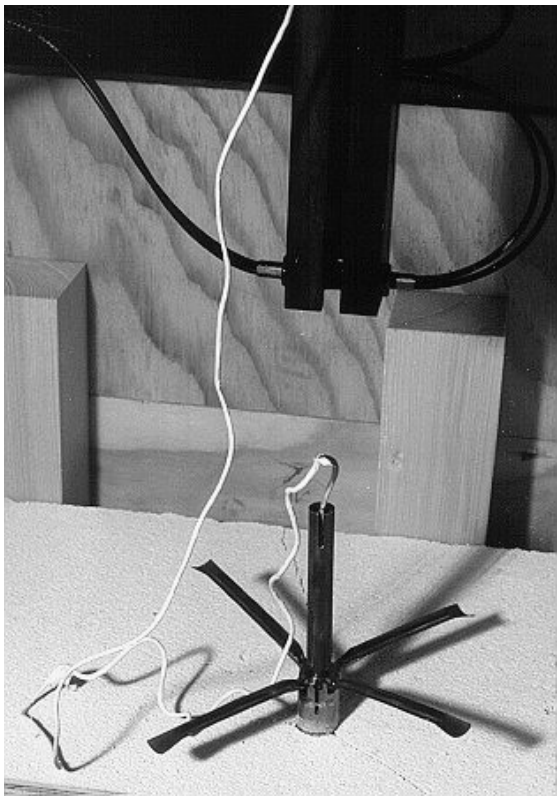

Figure 2 Penetration experiment in gas-concrete (14 MPa) using the anchor of the Rosetta Lander Philae

Fig. 1 shows the penetrometer test facility used for the quasi-static experiments. At the lower end it features an 18 mm diameter steel rod with 20 cm length and exchangeable load cells on both sides of the rod, where the lower sensor is called "Test Sensor" and the upper one is referred to as "Monitor Sensor". The force ranges available for this sensors are 25, 100, 500, and 1250 N. An exchangeable tip is mounted on the penetrometer rod just below the lower sensor. For our experiments we could choose between five different tip geometries, namely 30°, 45° and 60° opening angle cones, a half sphere and a flat cylindrical tip.

1.2 Dynamic penetrometry experiments

Dynamic penetrometry is the fast insertion of a projectile into soil where usually the deceleration of the projectile is measured.

By integrating over the signal we can derive impact speed and depth, which subsequently can be used in a dynamical soil model [5, 6].

A typical application of this technique in space exploration is the anchoring device of the Philae (Rosetta) Lander and the ACC-E penetration

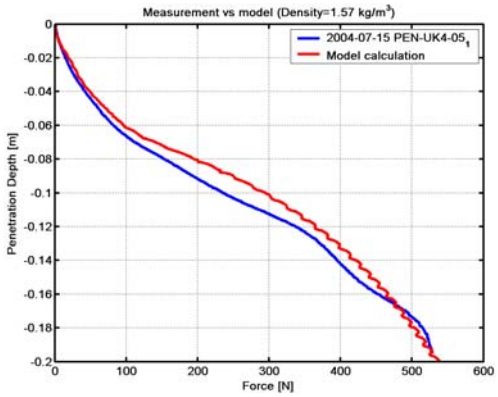

Figure 3 Relation of insertion force to penetrated depth for a measurement (lower) and a model calculation (upper). The major difference between the model and the calculation is due to the assumption of homogeneous sample properties for the model

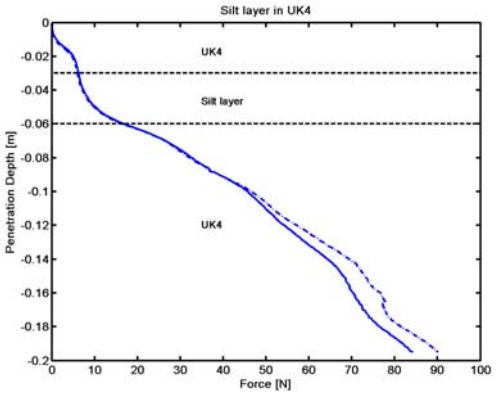

Figure 4 Example of a silt layer embedded within a UK4 sand with was compacted to an average bulk density of ~1400 kgm^{-3} whereas the silt layer had a bulk density of about 950 kgm^{-3}.

sensor of the Huygens Probe Surface Science Package.

For the development of the former we did many shots into target materials in the hardness range of comet materials from soft porous ice up to porous concrete with a crushing strength of ~14 MPa.

2 Penetrometry experiments

The result of a typical quasi-static penetrometry experiment is the relation of force versus depth, as can be seen in Fig. 3. The difference between the curves is that the lower curve is measured and the upper a model calculation from a finite element model using an extended Drucker-Prager constitutive model mostly used for frictional granular-like soils and rocks[4].

A granular sample is usually assembled by adding layers of sand and compacting them layer by layer in a predefined procedure which should ensure more or less homogeneous material parameters throughout the sample. However, a manual assembly of a dry granular sample requires a lot of experience and small discontinuities cannot be avoided. As can be seen in Fig. 3 from 13 - 16 cm depth a softer layer due to less compaction is detected within the sample and in Fig. 4 we put a 3 cm silt layer in a UK4 sand sample, which itself had density variations in its layers.

The difference in Fig. 4 between the solid and dashed curve is the location of the sensors. The upper sensor is also sampling the force due to shaft friction along the wetted surface of the penetrometer.

The detection of layering in penetrometry data still leaves some possibilities for explanation with a soil model. It could be a density variation, which is in the case of the example in Fig. 4 one factor, but it could be also a variation in the Youngs modulus due to a change in the sample mixture or a solidification process.

In the case of arid regions we can expect the formation of a duricrust i.e. a surface cementation due to chemical reactions in the top soil as a weathering product. Such a crust would be in the range of a couple of centimetres, and can easily be detected with penetrometry methods.

3 Small scale structure detection

As shown above, penetrometry experiments are valuable to calibrate input parameters for soil models and to detect local texture properties like layering or surface crusts. However, our aim was to demonstrate that a more thorough examination of the fine-structure of the penetrometry data can reveal more details of the investigated material.

If we postulate a very simple relationship between a regularly spaced structure and the speed we pass along this structure we can define the excited frequency as [8]:

$$f = \frac{v}{l} \qquad \text{(Eq. 1)}$$

where f is the excited frequency, v is the speed we move along, and l is a typical size scale of this structure. The principle is like moving along a picket fence with a stick in the hand. If we know

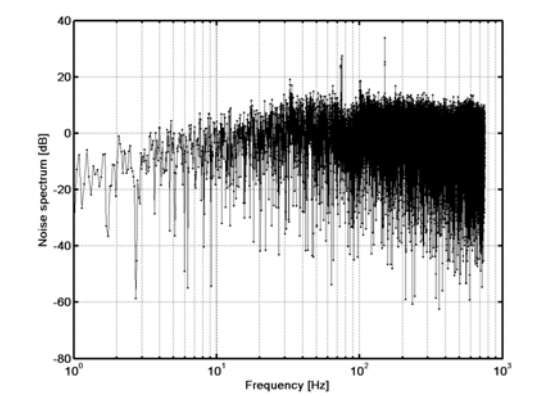

Figure 5 Noise spectrum of a quasi-static penetrometry experiment. The spectrum is normalized to 2σ standard deviation. For the count statistics typically the 500 largest positive frequency peaks are selected.

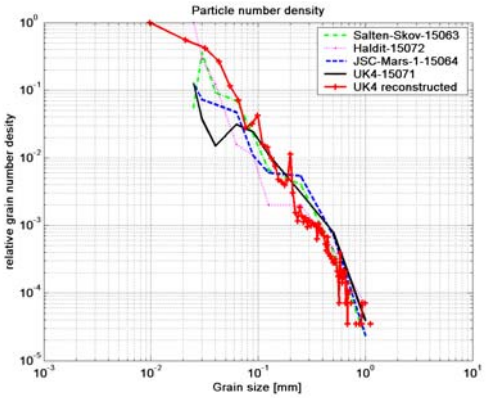

Figure 6 Grain number density of Martian analogue materials, derived with classical sieving methods. The reconstructed grain number is derived with the method described in the text.

the speed and record the rattling signal we can derive the spacing of the pickets.

A similar approach can be used for penetrometry experiments. However, we need to be aware that in this case we usually do not have completely regular structures. Yet, if we assume that a sample of granular material is more or less uniformly and homogeneously mixed and any small volume contains a representative amount of grains of all sizes, we can apply some statistical methods to derive a grain size distribution.

Geometrically, our picket fence contains now pickets which are no longer equally spaced. Still, the signal we are recording allows a determination of the width of every single picket in this one-dimensional example.

If we examine now the geometry of a penetrometer cone interaction with the soil, we can see that at any time a certain number of grains of different size collides with the cone causing a small reaction force on the penetrometer. The sum of all these small forces can be seen as noise superimposed on the total penetration resistance signal.

For a general evaluation of the total soil strength and for modelling purposes this noise is usually removed from the signal. However, if we want to analyse the fine structure of the sample we need to concentrate mainly on the noise present in the signal.

For this purpose we examine the frequency spectrum of the noise. Generally, we can distinguish between two sources for the noise. The first one is of course due to instrumental influences like ambient electric noise, e.g. a mains hum superimposed on the signal, and digitisation noise depending on the bit resolution of the sampling device. Also mechanical noise originating from the test rig may be present to some extent. All these systematic noise sources have to be carefully suppressed prior to a spectral analysis, otherwise the result will contain some unwanted contributions.

The second source of noise comes directly from the texture of the investigated sample material. If we now compute a noise spectrum (Fig. 5) which is free from systematic noise, we can use Eq. 1 to derive typical sizes from the N ($N=500$) most prominent frequency peaks. If we do some binning of these sizes we can obtain counting statistics which is representative for the grain size distribution of the penetrated soil (Fig. 6).

The use of multiple experiment data improves the counting statistics, because the occurrence of larger particles within a given sample volume is some orders of magnitude lower than that of smaller ones and thus more samples increase the statistical significance of the large grain counts.

Small grains are more numerous; however, they do not contribute as much to the total mass of the sample for this kind of Martian soil analogue materials.

The grain number density plot in Fig. 6 is however, not the best way to show the grain size distribution. For engineering applications, the grain size distribution of any granular soil sample is usually depicted in a cumulative weight ratio plot.

This kind of plot is a natural expression of the sieving procedure where a soil sample is put through a series of progressively finer meshes. The residual material within a certain mesh is then weighed and the cumulative mass over grain size plot is then normalized to the total mass of the sample.

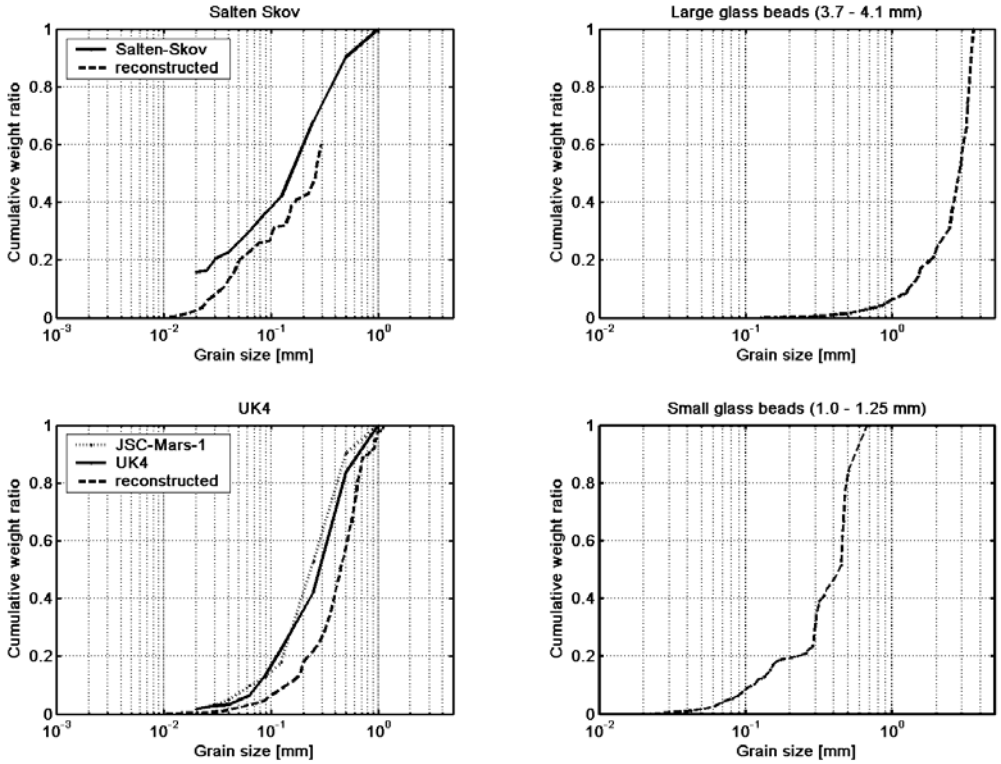

Figure 7 Reconstructed grain size distributions of Martian soil analogue materials (left panels) and glass beads with diameters of ~1 and ~4 mm diameter (right panels). The reconstructed material is indicated in the title of the respective panel.

In order to plot the reconstructed grain size distribution the number of grains of a certain size is multiplied by the mass of the grain. For simplicity the grains are assumed to be spherical. Thus the mass m_g of such a grain is then:

$$m_g = \frac{\pi}{6} d^3 \rho_g \qquad \text{(Eq. 2)}$$

Where d is the grain diameter and ρ_g is the grain density. Since the resulting cumulative mass is normalized the density can be arbitrarily set to 1 if only the bulk density of the sample material is known.

Using Eq. 2 and multiplying it with the grain number density N_g we can plot the reconstructed grain size distribution (Fig. 7). The two left panels of Fig. 7 show grain size distributions of a granular Martian analogue material.

It should be noted that especially in the upper left panel (Salten Skov material) the reconstructed curve can not match the sieve line result entirely. Because of an insufficient count of the fine grained particle fraction which is in total contributing approximately ~15% of the mass of this granular material. The reason for this fact is that the smallest grain population cannot be resolved due to a too low sampling rate and sensitivity of the load cell sensor.

Thus, for this material we have to be content with the fact that the general slope of the curve is in good agreement with the classically achieved result, but there is no way of matching the contribution of a population this method cannot resolve.

A much better agreement can be obtained for the other granular material in this plot (UK4, lower left panel), where the smallest grain population does not contribute more than ~2% of the total mass. Generally the discrepancy between the classical result and reconstruction is at maximum 20% but mostly even less.

On the right the panels of Fig. 7 we applied this method to glass beads of a more uniform grain size, namely to beads with a typical diameter of 3.7 - 4.1 mm (upper right panel) and beads with a typical diameter of 1.0 -1.25 mm. The accuracy of those diameters is however quite limited, since the original purpose of those glass beads is a usage as sanding agent. A close examination showed also a lot of elliptic particles within the sample, which

Property	Foamglas T4	Foamglas F
Bulk density [kgm^{-3}]	120	165
Porosity [%]	95	93
Nominal crushing strength [MPa]	0.85	1.70
Quasi-static penetration resistance [MPa]	0.8 - 1.8	3.0 - 4.5
Cell size (min, mean, max), [mm]	0.9, 1.6, 3.	0.8, 1.6, 3.1

Table 1, Bulk properties of FOAMGLAS ®.

would mimic particles with smaller diameter for this kind of spectral analysis.
The reconstruction result for the larger particles gave a maximum diameter of 3.6 mm and 80% of the total mass within particles larger than 2 mm diameter. For the smaller glass beads we obtained a largest reconstructed diameter of 0.7 mm and 80% of the mass within diameters larger than ~0.3 mm.

4 Analysis of dynamic impacts

In the analysis of data from the anchoring device of the Philae Lander we can follow a similar approach as for the quasi-static penetrometry. We can also use frequencies we observe within the noise spectra of the signal to relate them to size scales of the target material.
A major difference in the target material was that most of the anchor tests were not made with a granular target, but rather the opposite in a cohesive cellular material, namely foamed glass.
The reason for the use of such a material, was the unlimited availability and the reproducibility of the sample properties, which were essential for this kind of tests. For the two used qualities of "FOAMGLAS ®" the soft T4 and the harder F, we knew the bulk density, the nominal crushing strength, and to a more limited accuracy the averaged pore size and the bulk porosity (Table 1)[7].
A close investigation of the acceleration data showed that the anchor projectile features a

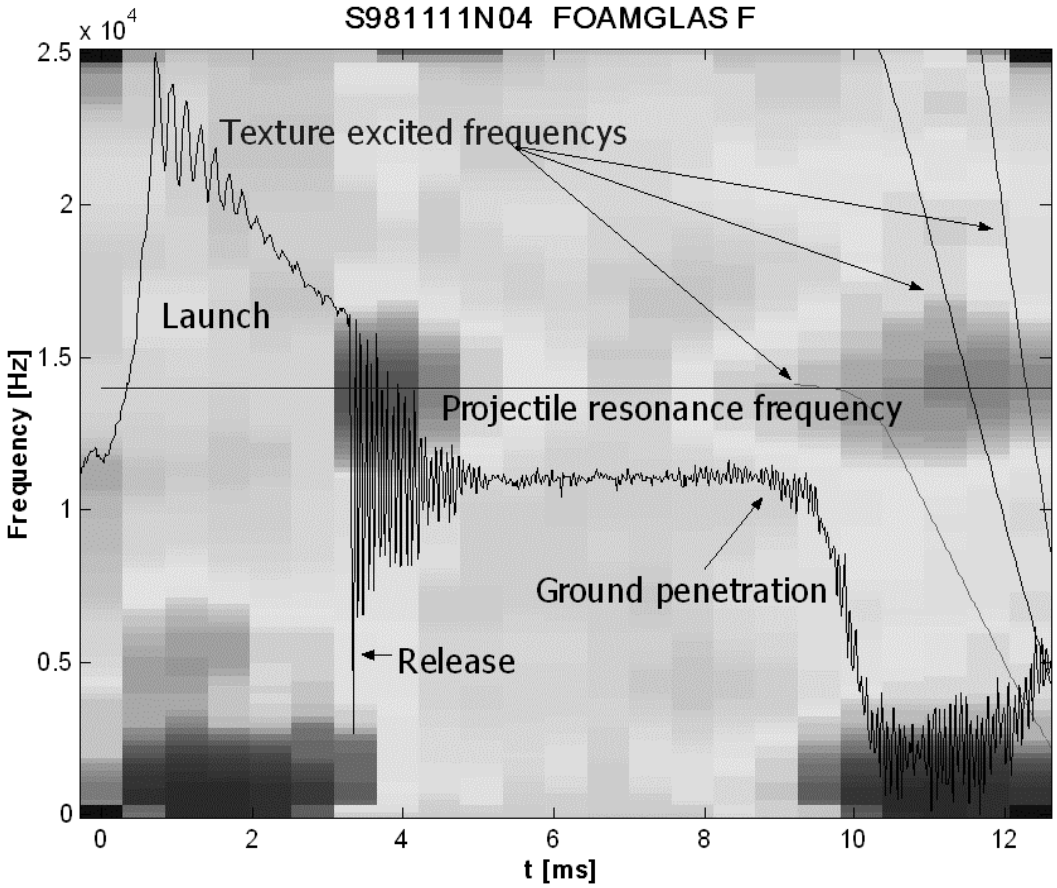

Figure 8 Spectrogram of the acceleration data of a test shot into a hard Foamglas target. Superimposed on the spectrogram are the acceleration data and frequency trails of cell induced frequencies during target penetration. In regions where the cell induced frequencies are suitably close to the projectile resonance, this resonant projectile ringing becomes excited too and thus can be detected in the signal.

resonant structural ringing at ~14 kHz, which was also confirmed by a numerical analysis of the projectile geometry [7,8].

We compute now a spectrogram of the anchor projectile acceleration data (Fig. 8) and then superimpose the trail of frequencies that would be caused by cell size effects of structures with diameters taken from Table 1 and the speed derived from integrating the deceleration signal (ref. Eq.1). It shows that in regions where the cell induced frequencies are close to the projectile resonance frequency, the projectile resonance is excited and is raising the noise level of the acceleration signal.

By comparing the cell sizes given for the glass foam (Table 1), we can see that the lower and upper size limit for the cell size is nicely bracketing the area of enhanced projectile resonant ringing.

A similar excitation of the projectile resonant ringing can be seen at the time of the release of the projectile from the launch tube, where we can see that without excitation mechanism the ringing is decaying within 1-2 ms.

Similar resonant ringing was seen also for the softer glass foam and other target materials like sand or porous water ice. However, since the forces involved for these softer materials are lower, the resonant ringing is less prominent but still identifiable with a lesser degree of accuracy [8,9].

5 Acknowledgements

We want to acknowledge that this work was funded by the Austrian Space Agency grant ASAP-CO-007/03 SPICE and supported by a Royal Society ESEP Joint Project Grant.

6 References

[1] J.C. Zarnecki, M.R. Leese, B. Hathi, A.J. Ball, A. Hagermann, M.C. Towner, R.D. Lorenz, J.A.M. McDonnell, S.F. Green, M.R. Patel, T.J. Ringrose, P.D. Rosenberg, K.R. Atkinson, M.D. Paton, M. Banaszkiewicz, B.C. Clark, F. Ferri, M. Fulchignoni, N.A.L. Ghafoor, G. Kargl, H. Svedhem, J. Delderfield, M. Grande, D.J. Parker, P.G. Challenor & J.E. Geake. A soft solid surface on Titan at the Huygens landing site as measured by the Surface Science Package (SSP), Nature, submitted, 2005

[2] Kömle N.I., Kargl G., Seiferlin K., Marczewski W., Measuring Thermo Mechanical Properties of Cometary Surfaces: In Situ Methods. *Earth Moon Planets*, 90, 269-282, 2002.

[3] J.C. Zarnecki, M. Banaszkiewicz, M. Bannister, W.V. Boynton, P. Challenor, B. Clark, P.M. Daniell, J. Delderfield, M.A. English, M. Fulchignoni, J.R.C. Garry, J.E. Geake, S.F. Green, B. Hathi, S. Jaroslawski, M.R. Leese, R.D. Lorenz, J.A.M. McDonnell, N. Merrywether-Clarke, C.S. Mill, R.J. Miller, G. Newton, D.J. Parker, P. Rabetts, H. Svedhem, R.F. Turner & M.J. Wright, The Huygens Surface Science Package. In Huygens: Science, payload and Mission, ESA SP-1177, 177-195, 1997.

[4] Zöhrer, A., Kargl, G."Finite Element Modelling of Penetration Tests into Martian analogue Materials" *Proceedings of the 3rd International Planetary Probe Workshop*, Anavyssos, Greece, 27.06. – 01.07.05.

[5] Christensen, P.R.; Moore, H.L., *The Martian Surface Layers*, Mars, Kieffer et al. (Eds.), University of Arizona Press, 686-729, 1992.

[6] J. B Johnson, A physically based penetration equation for compressible materials, *Penetrometry in the Solar System*, Kömle N.I., Kargl G., Ball A.J., Lorenz R.D. (Eds.), Austrian Academy of Sciences Press, 2001.

[7] Kömle N.I., Ball A.J., Kargl G., Keller T., Macher W., Thiel M., Stöcker J, and Rohe C., Impact penetrometry on a comet nucleus - interpretation of laboratory data using penetration models., *Planetary and Space Science*, 49, 575-598, 2001

[8] Kargl G., Kömle N.I, and Keller T., Interpretation of penetrometry experiments. *Penetrometry in the Solar System*, Kömle N.I., Kargl G., Ball A.J., Lorenz R.D. (Eds.), Austrian Academy of Sciences Press, 2001.

[9] Kargl, G., Macher W., Kömle N.I., Thiel M, Rohe C., Ball A.J., Accelerometry measurements using the Rosetta Lander's anchoring harpoon: experimental set-up, data reduction and signal analysis, *Planetary and Space Science*, 49, 425-435, 2001